Features of numerical modeling electrical coalescence in a droplet-layer system using the arbitrary Lagrangian-Eulerian method

Features of numerical modeling electrical coalescence in a droplet-layer system using the arbitrary Lagrangian-Eulerian method

I A Elagin, G S Yagodin and V A Chirkov
St. Petersburg State University, St. Petersburg, Russia

i.elagin@spbu.ru

Abstract. The electrocoalescence of a water drop at the water-oil interface was numerically analyzed using the finite element method by solving a set of equations including hydrodynamics and electrostatics. The simulation was performed using COMSOL Multiphysics software, the interface movement was implemented using an arbitrary Lagrangian-Eulerian method (also called the moving-mesh method). The influence of the initial distance from the drop to the layer, as well as the size of the entire domain on the outcome of the process was studied. The electrical coalescence and non-coalescence of a single uncharged droplet with a layer under the action of the DC field were calculated in a wide range of electric field strength. The created computer model makes it possible to calculate the voltage dependence of the detached droplet volume and charge. Also, it can help to determine features of non-coalescence, including the stretching of the droplet along the interelectrode gap and spraying.

1. Introduction

Mathematical modeling of electrohydrodynamical phenomena in two-phase immiscible liquids is a complicated multiphysics problem. Over the past few years, there has been a rapid development of the corresponding numerical models [1-3] but the solution of many problems is still unavailable for most researchers. In particular, the computation of the electrocoalescence processes between a drop suspended in oil and a layer of water is an underinvestigated problem, whereas this type of interaction is realized in many electrocoalescers [4]. This study concerns the features of modeling the corresponding process based on the Lagrangian-Eulerian method [5-7] (also referred to as the moving-mesh one). The possibility of using this approach to calculate electrical coalescence process for a two-drop system has only recently been proved [8]. A feature of the calculation of the problem by this method is the manual construction or tearing of bridge connecting volumes of liquids when there are prerequisites for a change in topology.

The dehydration procedure in the case of a "drop-layer" interaction is a process, in which many water droplets of various sizes located in an oil medium settle to the bottom of the coalescer under the action of gravity, as well as under the action of forces from an external electric field. A layer of water forms at the bottom of the device, which participates in the process of droplet coalescence. The presence of an electric field in the system is due to the presence of a high-voltage electrode, which is necessary to combine droplets into larger ones. In addition, in such systems, electric fields can be specially used to accelerate the film thinning process [9]. In this paper, we consider only a single drop settling on a layer

of water. As proof of the reliability of the developed model, the interaction of a drop with a layer of water at various external electric field strengths was compared with experimental works.

2. Model description

All simulations in this article were performed using COMSOL Multiphysics software version 5.4. The droplet-layer system consists of 3 parts: a spherical drop, the liquid surrounding it—oil, and a layer of water at the bottom of the system (figure 1). The problem has axial symmetry. For definiteness, we assume that the simulated volume of the fluid has the shape of a cylinder. The use of symmetry allows to reduce the calculation time as well as the cost of RAM.

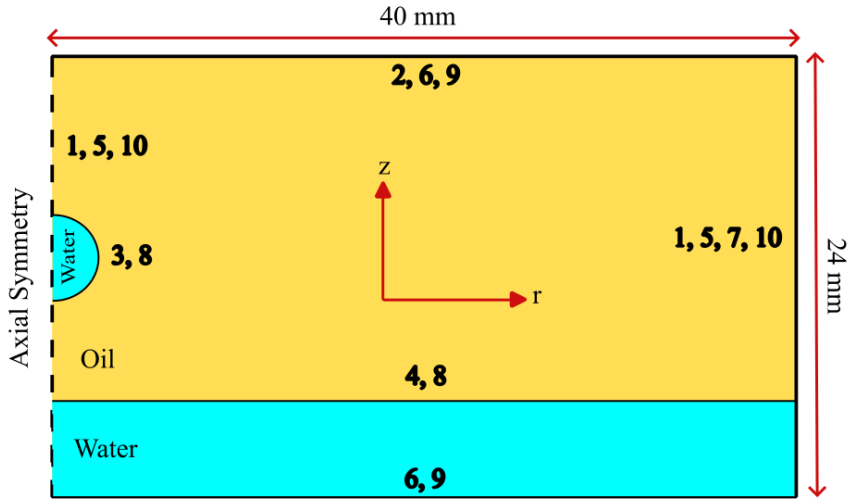

Figure 1. Geometry and boundary conditions of the problem.

Hydrodynamics is calculated in all domains of the model. The following hydrodynamic equations were used: the Navier-Stokes equation for the incompressible isothermal fluid (1), which includes gravity force, as well as the continuity equation for an incompressible fluid (2). In the case when the permittivity and conductivity of one medium (in this case water) significantly exceeds the permittivity of another medium (oil), it can be assumed that the first medium is the conductor [10]. If a charge emerges in such a system, for example, when an electric field is turned on, then it will be distributed strictly along the boundary of the conducting medium. Thus, the field inside will be practically absent. Consequently, the equation of electrostatics (3) can be solved only in the domain with oil.

$$\rho\frac{\partial \boldsymbol{v}}{\partial t} + \rho(\boldsymbol{v}\nabla)\boldsymbol{v} = -\nabla P + \mu\Delta\boldsymbol{v} + \rho\boldsymbol{g} \quad (1)$$

$$div\,\boldsymbol{v} = 0 \quad (2)$$

$$div(\varepsilon\varepsilon_0\boldsymbol{E}) = 0 \quad (3)$$

$$\boldsymbol{E} = -\nabla V \quad (4)$$

Here ρ is the liquid density, $\vec{v}$ is the velocity vector, t is the time, P is the pressure, g is the free-fall acceleration, τ is the Maxwell relaxation time, σ is the medium electrical conductivity, $\boldsymbol{E}$ is the electric field strength, V is the electric field potential, and μ is the dynamic viscosity.

Table 1. Boundary conditions.

Boundary condition	*Numeration*	*Mathematical form*	*Symbols meaning*
Electrostatics			
Axial symmetry, zero charge	1	$\boldsymbol{E}\cdot\boldsymbol{n}=0$	$\boldsymbol{n}$ is the normal to the surface
HV electrode potential	2	$\mathrm{V}=const$	
Floating potential	3	$\mathrm{V}=const,\quad \int_{\partial\Omega}(\boldsymbol{E}\cdot\boldsymbol{n})dS=Q=0$	Ω is the integration surface
LV electrode potential	4	$\mathrm{V}=0$	
Hydrodynamics			
Axial symmetry for velocity	5	$\boldsymbol{v}\cdot\boldsymbol{n}=0$	
No slip	6	$\boldsymbol{v}=0$	
Navier slip	7	$\boldsymbol{K_n}-(\boldsymbol{K_n}\cdot\boldsymbol{n})\boldsymbol{n}=-\frac{\mu}{\beta}(\boldsymbol{v}-(\boldsymbol{v}\cdot\boldsymbol{n})\boldsymbol{n})$ $\boldsymbol{K_n}=\mu(\nabla v+(\nabla v)^T)\boldsymbol{n}$	
Fluid-fluid interface	8	$\boldsymbol{n}\cdot(\boldsymbol{p_1}-\boldsymbol{p_2})=-p_e\boldsymbol{n}+\gamma(\nabla_t\cdot\boldsymbol{n})\boldsymbol{n}-\nabla_t\gamma$ $p_e=\frac{1}{2}\varepsilon\varepsilon_0E_n^2$	$\boldsymbol{p_1},\boldsymbol{p_2}$ **are** pressure inside and outside the droplet, p_e is the electrostatic pressure
Moving mesh			
Fixed boundary	9	$\boldsymbol{v}_{mesh}=0$	$\boldsymbol{v}_{mesh}$ is the velocity of mesh nodes
Symmetry/Roller	10	$\boldsymbol{v}_{mesh}\cdot\boldsymbol{n}=0$	

The boundary conditions used in the model are shown in figure 1, and are also listed in table 1. In the case when the dielectric permittivity of the droplet significantly exceeds the dielectric permittivity of the medium located, it is possible to represent the boundary of the droplet as an equipotential surface [10]. Therefore, an equipotential condition 3 was set at the interface between the drop and the oil, which allows to fix the total charge on the drop. Also, this condition allows to change the potential value depending on the position of the drop relative to the electrodes. The interface condition 8 was set at the interface of oil and water phases, which takes into account the surface tension force $F_{st}=2\gamma H$ (where γ is the interfacial tension, H is the mean curvature of the surface), as well as the electrostatic pressure p_e. Navier slip condition 7 was set on the right wall, which allows include the friction force $\boldsymbol{F}_{fr}=-\frac{\mu}{\beta}\boldsymbol{v_{tang}}$ (where $\boldsymbol{v_{tang}}$ is the tangential component of the velocity of the liquid on the wall, β is the coefficient having the meaning of the distance measured from the wall at which the velocity of the medium is zero). The need to use the "Navier slip" condition instead of the standard "No slip" arises from the fact that in COMSOL this is the only way the position of the right point of the layer boundary can move along the z axis (in case of moving mesh method). When the droplet and layer merge, the water level should rise, which leads to a shift of layer surface, including the rightmost point. It was found that fixing this point leads to a sharp increase of pressure in this area, which affects the stability of the solution.

The surface of the layer was fixed in such way that at any time it was perpendicular to the vessel wall. The perpendicularity of the layer boundary to the left wall is natural due to axial symmetry, but in order to fulfill the condition of perpendicularity on the right wall, it is necessary to choose a sufficiently large radial size of the model. Otherwise, an incorrect value of the angle between the wall and the layer leads to significant distortions of the line geometry of the layer.

The arbitrary Lagrangian-Eulerian (ALE) method was used to describe the motion of the phase boundaries. This method tracks the position of the boundary by moving the geometry line separating the two phases, and, as a consequence, the finite element mesh. In this method, the mesh elements locate along the boundary separating the phases (figure 2) and shifts with the geometry line. The equality of the velocities of both phases is set as boundary conditions on the interface surfaces, which ensures their

synchronous movement. The most optimal mesh build is achieved by splitting the drop boundary (radius 1 mm.) into 200 elements, the number of elements on the layer boundary is 500 (element ratio is 20), while the error in mesh convergence does not exceed 0.5%. The maximum size of the element inside the domains is 1 mm, with a maximum relative growth coefficient of 1.2. Also, quadratic geometry shape order is used in the model.

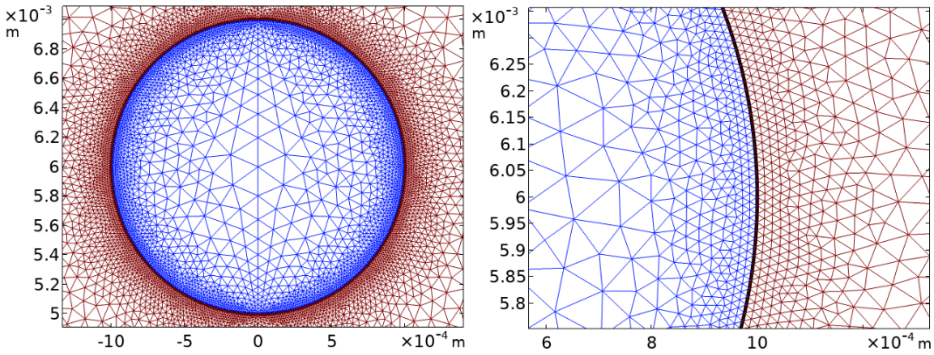

Figure 2. An example of a constructed mesh in the ALE method (on the left—a grid in the entire drop, on the right—an enlarged image near the interface area).

The ALE method allows to track the movement and deformation of the geometry line, but it is not suitable for describing problems with a changing topology. To calculate such problems, it is necessary to modify the method. The problem divides into 3 stages. At the first stage, the calculation of drowning a drop is performed until the distance between the surface of the drop and the layer becomes less than critical [11]. At the second stage, a manual construction of a bridge between two volumes of water is performed (figure 3). At stage 3, the problem is calculated with the geometry taken from stage 2 and modified boundary conditions (after the drop touches the layer, the surface of the drop and the layer have the same potential equal to 0). The initial distributions of the calculated values are taken from step 1. After that, the calculation continues until the drop is detached from the layer or until it is completely merged with the layer. It should be noted that at the stage 2 increased values of velocity and pressure gradients occur in the area near the bridge, so the mesh settings from the first stage are not suitable for the third stage. The boundary of the layer before the bridge was chosen to divide into 1000 elements with the element ratio of 80. The minimum size of the drop element was chosen to be 0.5 μm, the maximum 10 μm. The maximum size of the water domain element has been reduced by 4 times compared to the oil domain. This had to be done since the most intense fluid movement occurs in this area. Additionally, a point on the axis was created, it located at the same level with the surface of the layer. The element size was set on the line connecting this point and the tip of the drop: the maximum is 50 μm, the minimum is 1 μm. Conditions are also imposed on the bridge: the maximum element is 10 μm, the minimum is 0.5 μm, the maximum growth rate is 1.001. An example of the constructed mesh is shown in figure 3.

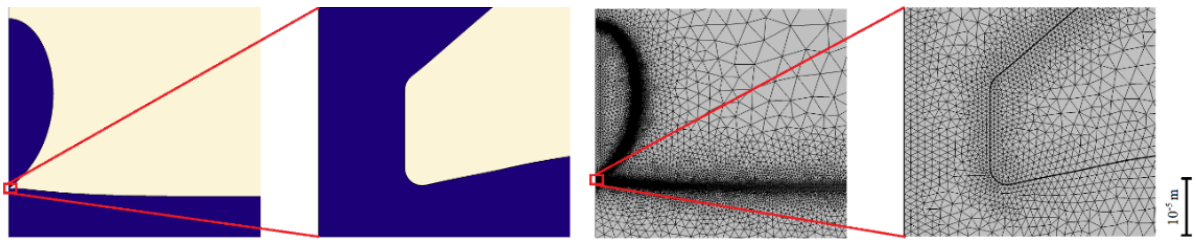

Figure 3. An example of a constructed bridge. A grid for calculating the 3d stage of the problem is demonstrated on the right-hand side.

The initial distance from the drop to the layer was chosen to be greater than 1 drop radius. According to figure 4, the average velocity of the drop at the moment of touch does not depend on the selected distance between drop and the layer (the height). Moreover, the distributions of the calculated values of velocity and potential are also identical, as shown in figure 5. At the beginning of its path, the drop accelerates mainly under the influence of gravity, as a result of which we observe an increase in speed. Then the drop begins to slow down due to the viscous friction forces, as well as due to the fact that it has to push the layers of oil at going to the bottom. When approaching the layer, the Coulomb forces begin to prevail, the drop starts to accelerate, while the area near the bridge acquires the maximum speed (figure 5).

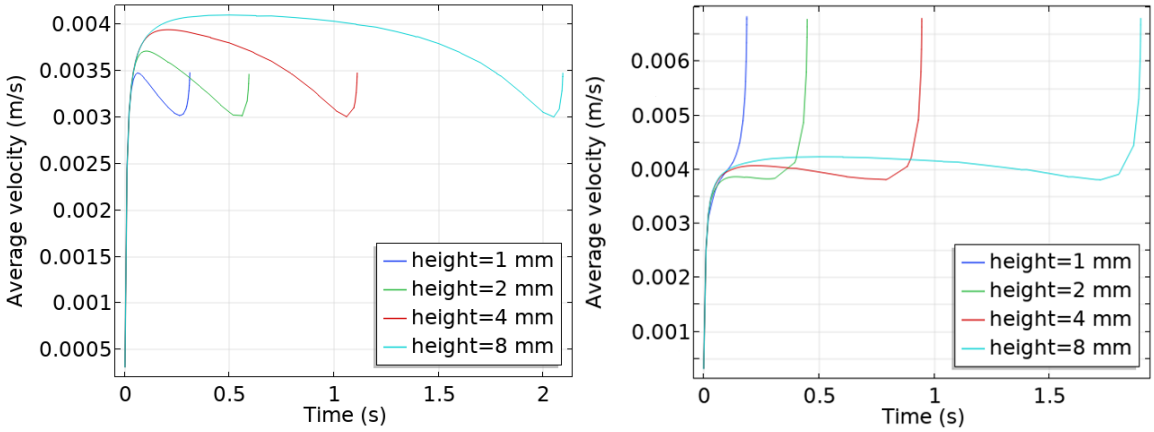

Figure 4. Dependences of the average drop velocity on time. Different colors indicate different initial height of the drop above the layer. R = 1 mm, E = 1 kV/cm (on the left) and E = 2 kV/cm (on the right).

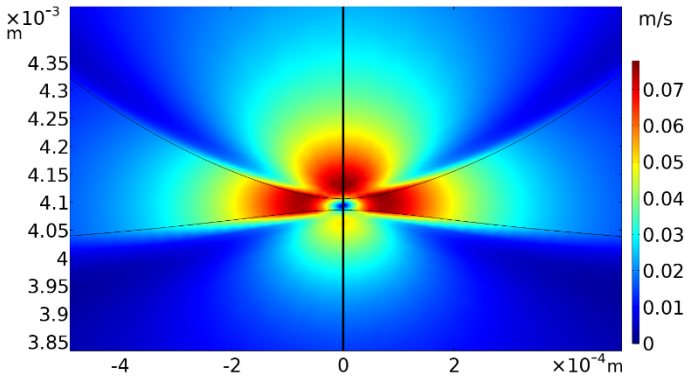

Figure 5. Contour plot of the velocity at the moment before drop touched the layer. Presented on the left part of the figure is a drop drowning from a height of 2 mm above the layer, whereas on the right—a drop drowning from a height of 8 mm.

3. Results

The simulation was performed for olive oil with the characteristics: density ρ = 910 kg/m^3, dynamic viscosity η = 0.065 Pa · s, relative permittivity ε = 2.85. Water was taken as the drop and the layer material ρ = 1000 kg/m^3, η = 0.001 Pa · s. The interfacial tension between water and oil is equal to γ = 0.016 N/m.

As a result of the simulation, three possible outcomes were obtained: complete coalescence, partial coalescence and stretching along the interelectrode gap. The outcome of coalescence depends only on the value of the applied electric field strength. At low electric field strengths (less than 1.2 kV/cm), a

complete union of a drop with a layer (coalescence) was observed. In this mode, the Coulomb forces are small enough compared to the surface tension force to tear the drop off the water surface, so their fusion occurs as shown in figure 6 (a). As the tension increases, the Coulomb forces also increase. Therefore, when the threshold (1.2 ± 0.1) kV/cm is crossed, a daughter drop begins to separate from the layer (figure 6 (b), (c)), the volume of which is proportional to the applied field (the characteristic dependence of the radius of the daughter drop on the applied electric field is shown in figure 7). At electric field strengths above $E = (3.3 \pm 0.1)$ kV/cm, the process of stretching along the interelectrode gap was observed. This process is characterized by the fact that the tip of the droplet acquires a high velocity directed to the upper electrode (the arrows in figure 8 show the direction of fluid velocity), while the bridge narrows much slower than in the case of partial coalescence. This process may be accompanied by a sharpening of the tip of the drop due to its upward movement. This sharpening leads to the fact that the electric field intensity increases (figure 8) and, as a result, the formation of a small drop begins to occur, which can separate from the main one. Thus, in addition to the potential closure of the interelectrode gap, this case is dangerous because the average volume of droplets in the emulsion decreases. This mode is shown in figure 6 (c). It is worth noting that the threshold of transition to spraying appears at the moment when the volume of the daughter drop is almost equal to the initial volume of the drop, as can be seen from figure 7.

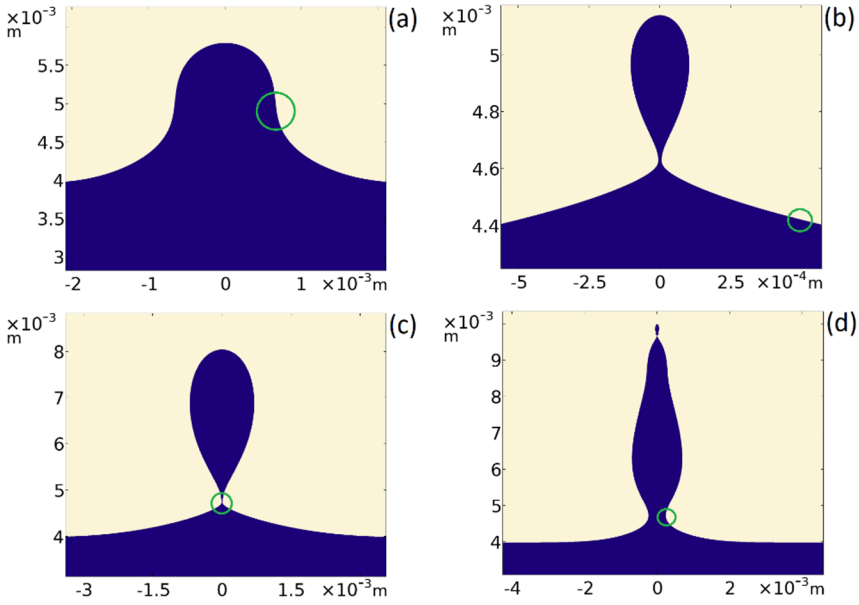

Figure 6. (a) Example of coalescence (E = 1 kV/cm, R = 1 mm, not the final moment of calculation). (b) Example of partial coalescence (E = 1.6 kV/cm, R = 1 mm). (c) Example of partial coalescence (E = 3 kV/cm, R = 1 mm). (d) Example of stretching along the interelectrode gap (E = 3.6 kV/cm, R = 1 mm). The green circle marks the position of the bridge surface at the end of the calculation.

It was found that the thinning of the bridge can occur both in the area of the bridge itself and above it, and the lower the applied voltage, the higher the narrowing area shifts (figures 6 (b)–(d)).

The three modes obtained were observed in a several experimental studies [3,9,12]. The dependence in figure 7 agrees well with the experimental data [9].

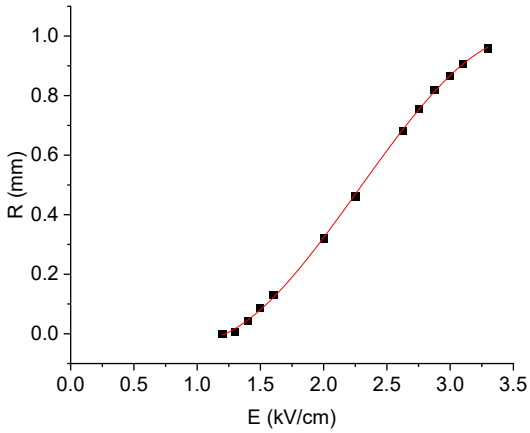

Figure 7 The dependence of the radius (volume was converted into radius) of the daughter drop on the average electric field strength, R = 1 mm.

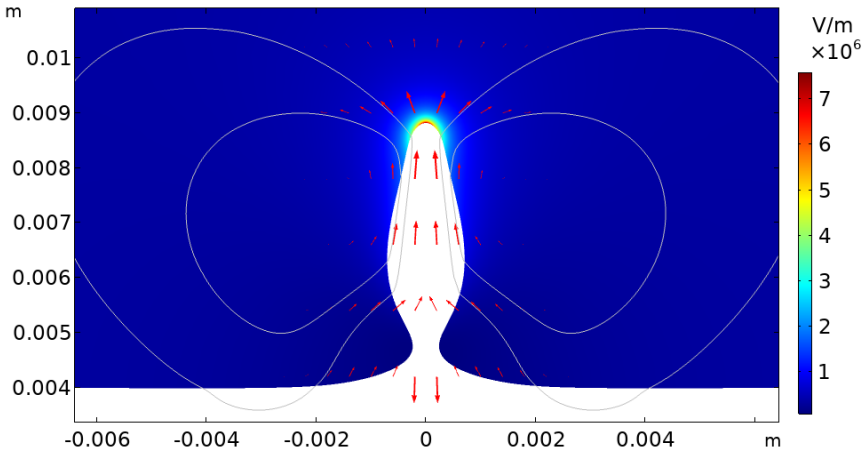

Figure 8. Contour graph of the electric field strength. The electric field strength is increased in the area above the drop. Arrows indicate velocity vectors, white lines - streamlines. Droplet moves to the HV electrode. E = 3.5 kV/cm, R = 1 mm.

4. Conclusion

The numerical model allows one to obtain all the outcomes previously described in experimental studies—complete and partial coalescence and non-coalescence. In the case of partial coalescence, the location of droplet separation from the layer does not always correspond to that of the initial water bridge and depends on the electric field strength. The created computer model makes it possible to calculate the voltage dependence of the detached droplet volume and charge. Also, it can help to determine features of non-coalescence, including the stretching of the droplet along the interelectrode gap and spraying.

Acknowledgments

The study was supported by Russian Science Foundation, research project No. 22-79-10078, https://rscf.ru/en/project/22-79-10078/. The research was performed at the Research park of St. Petersburg State University “Computing Center,” “Center for Nanofabrication of Photoactive Materials

(Nanophotonics),” and “Center for Diagnostics of Functional Materials for Medicine, Pharmacology, and Nanoelectronics.”

References

[1] Deka D and Pati S 2023 *J. Colloids Surf., A* **664** 131152
[2] Li B, Wang Z, Vivacqua V, Ghadiri M, Wang J, Zhang W, Wang D, Liu H, Sun Z and Wang Z 2020 *J. Chem. Eng. Sci.* **213** 115360
[3] Chirkov V A, Saifullin D D, Utiugov G O and Samusenko A V 2023 *5th International Youth Conference on Radio Electronics*, *Electrical and Power Engineering* (Moscow), IEEE pp 1-5
[4] Mhatre S, Vivacqua V, Ghadiri M, Abdullah A M, Al-Marri M J, Hassanpour A, Hewakandamby B, Azzopardi B and Kermani B 2015 *J. Chem. Eng. Res. Des.* **96** 177–195
[5] Hirt C W, Amsden A A and Cook J L 1974 *J. Comput. Phys.* **14** 227–253
[6] Supeene G, Koch C R and Bhattacharjee S 2008 *J. Colloid Interface Sci.* **318** 463–476
[7] Raisin J, Reboud J L and Atten P 2011 *J. J. Electrostat.* **69** 275–283
[8] Chirkov V A, Reznikova M P, Lashko A V and Dobrovolskii I A 2018 *2nd International Conference on Dielectrics* (Budapest), IEEE pp 1–4
[9] Mousavichoubeh M, Shariaty-Niassar M and Ghadiri M 2011 *J. Chem. Eng. Sci.* **66** 5330–5337
[10] Eow J S, Ghadiri M, Sharif A O and Williams T J 2001 *J. Chem. Eng. J.* **84** 173–192
[11] Utiugov G O, Chirkov V A and Dobrovolskii I A 2020 *3rd International Conference on Dielectrics* (Valencia), IEEE pp 529-532
[12] Hellesø S M, Atten P, Berg G and Lundgaard L E 2015 *J. Exp. Fluids* **56** 122